Available online at www.sciencedirect.com
ScienceDirect
Journal of the European Ceramic Society 27 (2007) 3753–3758
www.elsevier.com/locate/jeurceramsoc

Growth process approaches for improved properties of tunable ferroelectric thin films

Tomoaki Yamada*, Vladimir O. Sherman, Dong Su, Paul Muralt, Alexander K. Tagantsev, Nava Setter

Ceramics Laboratory, Swiss Federal Institute of Technology, EPFL, CH-1015 Lausanne, Switzerland

Available online 13 March 2007

Abstract

Two approaches are shown for property control of tunable $Ba_xSr_{1-x}TiO_3$ (BST) films: (i) two-step growth and (ii) self-selective epitaxial growth. Both processes are based on the deposition of an amorphous ultra thin BST layer prior to the growth of an epitaxial BST film. In the first approach, the mechanical strain in the epitaxial films is controlled by employing a two-step growth process, where the very thin amorphous layer deposited first acts as an absorption layer for the misfit strain through its crystallization. Two-step grown films on $LaAlO_3$ substrates showed effective relaxation of the compressive misfit strain, which resulted in higher in-plane permittivity and tunability of the film. In the second approach, self-selective epitaxial growth, epitaxial/amorphous BST composite structures are achieved where the two phases are electrically inter-connected in parallel. Having a low permittivity, the amorphous component efficiently suppressed the effective permittivity of the composite capacitor, while the epitaxial component helps keep the tunability as large as that of a purely epitaxial BST film. The resultant composite film demonstrated a low permittivity having a high tunability, which is the contradictory phenomenon for a pure tunable ferroelectric.

Keywords: Films; Nanocomposites; Dielectric properties; $BaTiO_3$ and titanates; Tunable property

1. Introduction

Tunable ferroelectric films have been intensively studied for a wide array of possible microwave applications.[1,2] Although the required properties of the films depend on the intended purposes, there are general requirements for microwave devices such as high tunability, low dielectric loss, intermediate (preferably low) capacitance and weak temperature dependence. However, since many properties are in fact inter-connected, one needs trade-off between them for the practical applications.

The main way to control the properties of a film is via its processing. In this paper, we introduce two new growth strategies for the property control of tunable $Ba_xSr_{1-x}TiO_3$ (BST) films toward an improved performance; namely, (i) two-step growth and (ii) self-selective epitaxial growth. Both growth processes utilize a thin amorphous BST layer, which has the same chemical composition as the film.

In the first approach, the mechanical strain in the epitaxial films is controlled using the first thin amorphous layer. This growth process allows us to modify the strain keeping the substrate, film thickness and deposition conditions unchanged. The difference in the strain finally leads to a significantly different permittivity and tunability of the film. In the second approach, epitaxial/amorphous composite film structures are fabricated. By patterning the first thin amorphous layer, simultaneous growth of epitaxial and amorphous BST phases is achieved on the same level. The fabricated composite structure leads to the reduction of the permittivity while keeping the high tunability of epitaxial films.

2. Experimental

Pulsed laser deposition with KrF excimer laser ($\lambda = 248$ nm) was used for the deposition of BST films. The laser energy and repetition rate were 220 mJ and 5–7 Hz, respectively. Ceramic disks of BST were used as targets which were made using the standard ceramic synthesis technique. As for the composition of BST, $x = 0$, i.e., $SrTiO_3$ (STO), and $x = 0.3$ were selected for the first and second growth approaches, respectively. The details

* Corresponding author at: Swiss Federal Institute of Technology, EPFL, STI-IMX-LC, MXD 210, Station 12, Lausanne CH-1015, Switzerland.
Tel.: +41 21 693 4952; fax: +41 21 693 5810.
E-mail address: tomoaki.yamada@epfl.ch (T. Yamada).

0955-2219/$ – see front matter © 2007 Elsevier Ltd. All rights reserved.
doi:10.1016/j.jeurceramsoc.2007.02.027

of the growth conditions and process flows will be described afterwards.

The surface morphology and structure were observed by reflection high-energy electron diffraction (RHEED). The structural properties were characterized by X-ray diffraction (XRD) and by transmission electron microscopy (TEM). An HP 4284A precision LCR meter was used for low frequency dielectric measurements. For the microwave frequency measurements, the resonance method was used,[3] and the resonant frequency was about 8 GHz.

3. Results and discussion

3.1. Two-step growth: enhanced tunability by strain manipulation of epitaxial STO films

In a pure ferroelectric, the tunability is sensitive to the permittivity; therefore, a high permittivity is necessary to realize a high tunability. It has been experimentally and theoretically documented that the strain in an epitaxial ferroelectric film significantly affects its permittivity.[4,5] Commonly, the strain is controlled by using different growth conditions (such as growth/annealing temperature and gas pressure), film thicknesses, substrates and sub-layers of other compositions, although these may also influence other physical or chemical properties of the films. Here, we employed a so-called two-step growth process, which allowed us to modify the strain in the epitaxial films keeping these parameters unchanged.

Fig. 1 shows the deposition sequence for the two-step grown STO films. First, a very thin amorphous STO layer, less than 10 nm, was deposited on a $LaAlO_3$ (LAO) (1 0 0) single crystal substrate at 100 °C (Fig. 1(a)). After deposition of the first layer, the substrate was heated up to 750 °C and was kept at this temperature for some time (Fig. 1(b)). It can be expected that this annealing step leads to the epitaxial crystallization of the first layer. At the same time, crystallization from amorphous phase will result in effective relaxation of the strain from the lattice mismatch. Then, film growth proceeded at the same temperature as used for the annealing step until the desired film thickness was obtained (Fig. 1(c)). In this growth process, the thickness of the first layer can be used to control its impact.

A cube-on-cube epitaxial relationship was observed for both normally grown and two-step grown films. This supports the

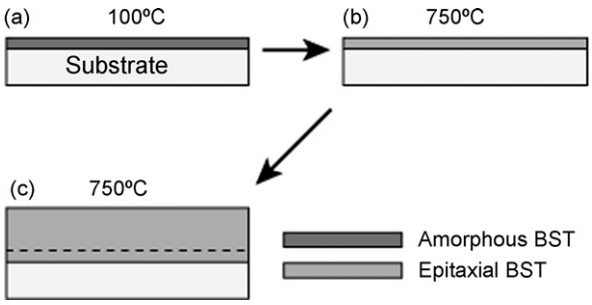

Fig. 1. Process flow of two-step grown films: deposition of the first thin amorphous STO layer at 100 °C (a), epitaxial crystallization of the fist layer at 750 °C (b), and deposition of STO film at 750 °C (c).

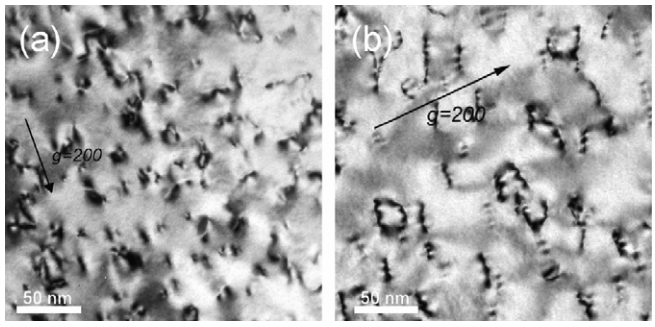

Fig. 2. Typical bright-field plan-view TEM images ($g = 200$) of the STO films excluding the film/substrate interfaces; without first layer (a) and with 5-nm thick first layer (b).

supposition that the amorphous first layer was epitaxially crystallized at a high temperature before the second layer deposition, as expected. In addition, no significant difference in the crystallinity was found in the XRD spectra for both films.[6]

Strain relaxation during the growth of epitaxial films will be strongly related to the formation of dislocations. Fig. 2 shows typical plan-view TEM images for the normally grown film and two-step grown film where the substrates (and film/substrate interfaces) were etched-off. A lower dislocation density was clearly observed for the two-step grown film. The difference in the dislocation density in the films can be explained as follows. In the case of the normally grown film, as in typically reported films, strain relaxation will occur via the nucleation of dislocation half-loops at the free surface of the growing film and their expansion to the interface by glide.[7] During growth, two or more generated half-loops are combined and form a long misfit dislocation line at the film/substrate interface with two threading dislocations passing through the film. This process consequently leads to the minimization of the dislocation density in the film, at the expense of a high misfit dislocation density at the interface. However, in the actual film, the relaxation proceeds very slowly because of a large activation barrier for the dislocation movement. Therefore, the threading dislocation density of the film will not be minimized unless the film becomes very thick. On the other hand, the situation is different for the two-step grown film. The first layer deposited at a low temperature may contain a number of defects that can work as nucleation sites for crystallization during the following annealing step at high temperature. During crystallization, the existing and generated dislocations may be combined and pushed out to the interface, which leads to effective strain relaxation. If the first layer is fully relaxed before depositing the second layer, new half loops are not generated during further deposition. Therefore, the minimization of the threading dislocation density can be expected. The results shown in Fig. 2 are in good agreement with this explanation. The details of the structural analysis (dislocation types and a presence of stacking faults) by TEM observations will be described elsewhere.

Fig. 3 shows the strain u of the 250-nm thick two-step grown films as a function of the thickness of the first layer. As can be seen, the film without the first layer, i.e., the normally grown film, is under compressive strain along the in-plane direction because

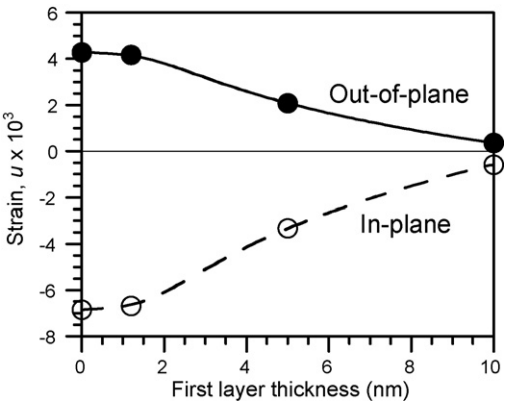

Fig. 3. Strain u of 250-nm thick two-step grown STO films with different first layer thickness at room temperature. The solid and dashed lines show the out-of-plane and in-plane strains. The in-plane strain of the films was estimated from the measured out-of-plane strain using the Poisson effect.

of a lattice mismatch of about −3% between the film and substrate. The compressive strain was significantly reduced with increasing thickness of the first layer, and it became nearly zero when a 10-nm thick first layer was used. The strain relaxation behavior during the growth by in situ RHEED monitoring[8] indicated that the 10-nm thick first layer was almost fully relaxed before deposition of the second layer. Our findings support a reduction of the threading dislocation density in the two-step grown films as observed by TEM.

The dielectric response of the films was tested in planar capacitor geometry with two rectangular Cu/Cr electrodes deposited onto the film surface. Here, the in-plane component of permittivity can be measured. The permittivity of the film was estimated from the measured capacitance using the partial capacitance method.[9] For all the films, no frequency dependence of the permittivity in the range of 10 kHz to 8 GHz was found, as reported for bulk STO. Fig. 4 shows the measured in-plane permittivity ε_{11} and tunability n of the films at 8 GHz and 168 K. As can be seen, the in-plane permittivity significantly increases

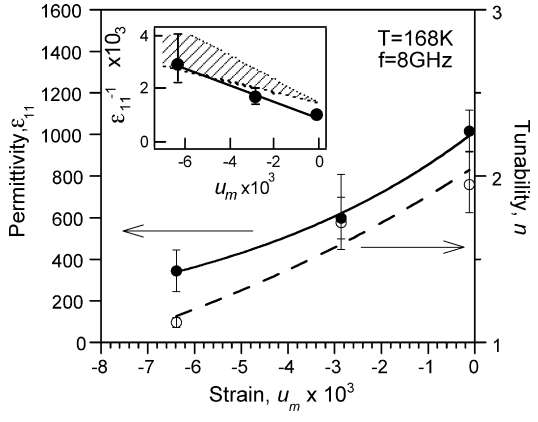

Fig. 4. Change of in-plane permittivity ε_{11} and tunability n (E = 140 kV/cm) with the different in-plane strain u_m in the two-step grown STO films measured at 168 K and 8 GHz. The strain at 168 K was estimated by considering the difference in the thermal expansion coefficients between STO film and LAO substrate. The inset shows the inverse in-plane permittivity ε_{11}^{-1} of the films. The hatched area shows the theoretical predictions obtained by Eq. (1).

with decreasing in-plane compressive strain using the first layer. As can been in the inset of Fig. 4, this trend agrees with the theoretical prediction based on Landau theory, expressed as

$$\varepsilon_{11}^{-1} = \varepsilon^{-1} - 2\varepsilon_0 \left(q_{11} + \left(1 - \frac{2c_{12}}{c_{11}} \right) q_{12} \right) u_m \quad (1)$$

where ε is the relative permittivity of unstrained STO, ε_0 is the permittivity of vacuum, q_{ij} is the component of the electrostrictive tensor of STO, c_{ij} is the elastic constant of STO, and u_m ($=u_1 = u_2$) is the in-plane strain in the film, respectively.[6] At the same time, the observed permittivities were somewhat higher than that expected. As for the tunability, at a high enough applied field E (namely, $n \gg 1$), it can be expressed by the relation:

$$n = \frac{\varepsilon(0)}{\varepsilon(E)} \approx 3\varepsilon_0 \varepsilon(0) \beta^{1/3} E^{2/3}, \quad (2)$$

where β is the coefficient of the dielectric nonlinearity. Since $n \propto \varepsilon(0)$, one can readily find a correlation between strain and tunability similar to that between strain and permittivity. As can be seen in Fig. 4, the tunability was also strongly enhanced by the strain relaxation in the same manner as the permittivity.

These results indicate that the amorphous first layer can be efficiently used for strain manipulation of the epitaxial ferroelectric films through its epitaxial crystallization. The relaxation of the compressive strain resulted in a high film permittivity. This in turn leads to enhancement of tunability.

3.2. Self-selective epitaxial growth: reduced permittivity without deterioration of the tunability of BST ($x = 0.3$) films

As mentioned above, a high permittivity is principally required to realize a high tunability in ferroelectrics. However, a small capacitance of the capacitor is often required for impedance matching in microwave devices. Although this can be achieved by designing the capacitor's geometry, one can expect that the realization of a reduced film permittivity while keeping the tunability unchanged will open possibilities for further applications.

One possible approach is to fabricate composite materials consisting of ferroelectrics with low-permittivity dielectric inclusions.[10] Particularly, in case that ferroelectrics and dielectric inclusions are electrically connected in parallel, i.e., in a parallel composite structure, one can expect to keep the tunability fairly unchanged even with a high concentration of inclusions. Therefore, only the effective permittivity can be significantly reduced. Herein, we experimentally demonstrate this effect by employing a selective epitaxial growth process for the fabrication of the said parallel composite structure. This growth process involves the self build-up of epitaxial/amorphous BST composite structures in which amorphous BST works as a low-permittivity dielectric component.

Fig. 5 shows the process flow for the fabrication of the composite structure. The BST ($x = 0.3$) films were deposited on STO (1 0 0) substrates electroded with epitaxial $SrRuO_3$ (SRO) (SRO[1 0 0]||STO[1 0 0]). First, a photo resist pattern having periodic strips (10–20 μm width) or circles (1–2 μm diameter) was fabricated on the surface by photolithography (Fig. 5(a)).

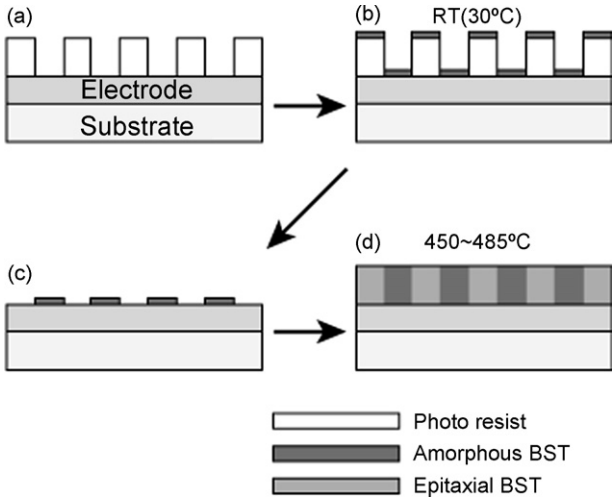

Fig. 5. Process flow of the composite structure by self-selective epitaxial growth: patterning of photo resist (a), deposition of thin amorphous BST ($x = 0.3$) layer at room temperature (30 °C) (b), lift-off (c), and deposition of BST ($x = 0.3$) film at 450–485 °C (d).

Subsequently, a 5–10-nm thick amorphous first BST layer was deposited onto the structured photo resist at room temperature under the base pressure of 10^{-8} Torr (Fig. 5(b)). The use of such a low pressure for the first layer deposition realizes the sharp pattering of the first layer. After lift-off, a patterned amorphous first layer was obtained on the monocrystalline electrode surface (Fig. 5(c)). Then, the 150-nm thick BST film was deposited onto the whole substrate at the temperature of 450–485 °C in 100 mTorr O_2 (Fig. 5(d)). 50 μm × 50 μm Pt top electrodes were deposited and annealed in air at 350 °C for 2 h.

Fig. 6 shows the RHEED image from the BST film directly grown on the epitaxial electrode surface. It was found that the cube-on-cube epitaxial growth of BST was clearly achieved at such a low deposition temperature, although BST films are commonly deposited at higher temperature. On the other hand, the BST film grown on the 7-nm thick first thin amorphous layer showed almost no diffractions, basically indicating its amorphous nature. These results indicate that the crystallization temperature of BST films is strongly affected by the underlying surface structure. Namely, the matched epitaxial surface leads

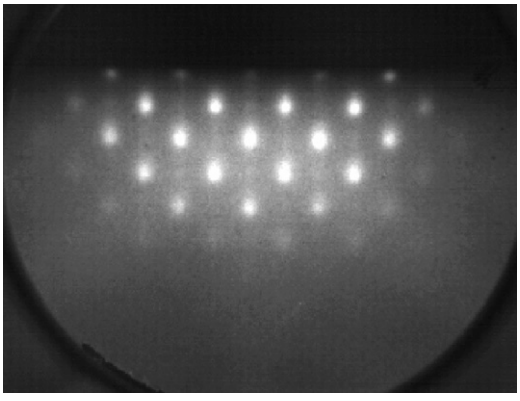

Fig. 6. RHEED image of BST ($x = 0.3$) film directly grown on epitaxial SRO electrode.

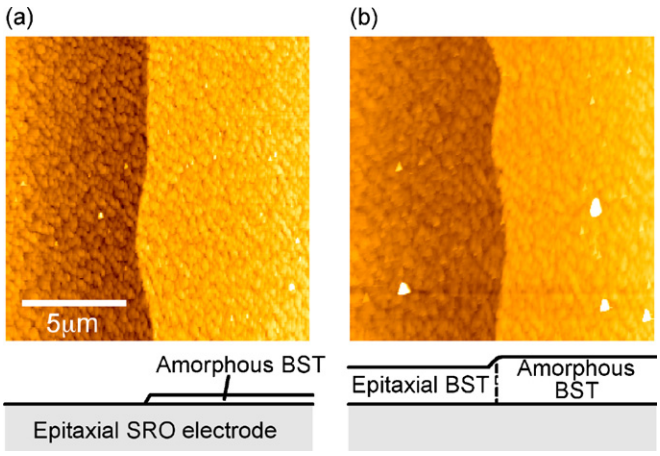

Fig. 7. AFM images (15 μm × 15 μm area) at the border of prepatterend first thin amorphous BST ($x = 0.3$) layer (a) and the similar area covered with BST ($x = 0.3$) film (b).

to low temperature epitaxial growth, whereas the amorphous surface blocks the crystallization of the growing film. This is compatible with the report stating that the crystallization temperature of BST films on LAO crystal is around 450 °C, but that on amorphous SiO_x is higher than 550 °C.[11] Consequently, by using a patterned, amorphous, thin first layer, the simultaneous growth of both epitaxial and amorphous BSTs occurs on the same level, which results in the self built-up composite film structure.

Fig. 7 shows AFM images of the border of the amorphous thin BST first layer and a similar area covered with the BST film. It can be seen that the fabricated composite structure showed sharp boundaries as observed for the patterned first layer. This indicates that, on the examined scale, the resolution of the patterning used defines the minimum feature size for the composite structure. Further scaling down will therefore be possible in the future.

Field dependence of the effective permittivity of the BST composite capacitors with different volume fraction q of the amorphous BST is shown in Fig. 8. It is expected that amorphous BST has a low permittivity because of its amorphicity; therefore it will work as a low-K dielectric component in the

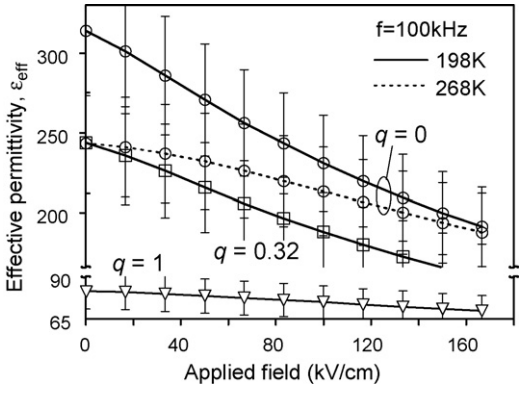

Fig. 8. Field dependence of the effective permittivity ε_{eff} of BST ($x = 0.3$) composite capacitors for $q = 0$, 0.32 and 1 at 100 KHz. The solid and dashed lines show the data measured at 198 and 268 K, respectively.

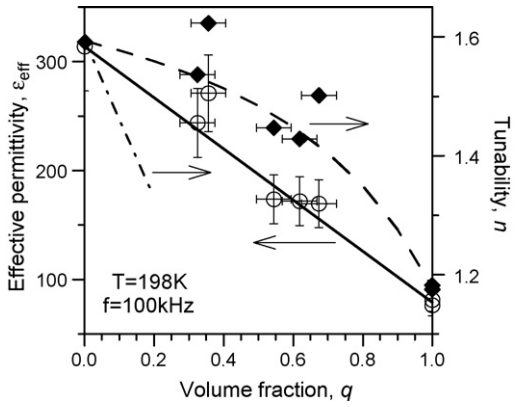

Fig. 9. Effective permittivity ε_{eff} and tunability n ($E = 166$ kV/cm) of BST ($x = 0.3$) composite capacitors with different q measured at 198 K and 100 kHz. The solid and dashed lines show the theoretical predictions of ε_{eff} and n for the parallel composite model, respectively. The dashed-dot line shows the estimation of n for a pure BST by taking the epitaxial BST capacitor ($q = 0$) as a standard.

composite structure. As can be seen, the epitaxial BST capacitor ($q = 0$) showed a high permittivity and a large field dependence, whereas the amorphous BST capacitor ($q = 1$) showed a significantly lower permittivity and a very weak field dependence. On the other hand, the composite capacitor ($q = 0.32$) showed an intermediate permittivity but a large field dependence similar to that for the epitaxial BST capacitor. Note that the tunability of the composite capacitor measured at 198 K is higher than that of the epitaxial BST capacitor measured at a higher temperature of 268 K, even though the both permittivities at zero dc field are same.

Fig. 9 shows the effective permittivity and tunability of the composite capacitors with different q. As can be seen, the measured effective permittivity linearly decreased with increasing q. On the other hand, the tunability decreased very slowly compared to the effective permittivity. The linear dependence of the effective permittivity ε_{eff} is given by the relation: $\varepsilon_{eff}(0) = \varepsilon_f(0)(1 - q) + \varepsilon_d(0)q$, where ε_f and ε_d are the permittivities of the ferroelectric and dielectric components, respectively. As for the tunability, since the dc field is equally applied to both components, the ferroelectric component is tuned as efficiently as a pure ferroelectric. The observed tunability accords with the theoretical prediction for the parallel composite model (see details of the equation in Ref. 12). For comparison with pure BST, the tunability calculated from the Eq. (2) by taking the epitaxial BST capacitor as a pure BST's standard is also plotted in Fig. 9. It is clear that the tunability of the fabricated composite cannot be explained by the behavior of pure ferroelectrics; namely, there is a good separation between both epitaxial/amorphous BST phases.

The obtained results indicate that the selective epitaxial growth process can be useful for the fabrication of the parallel composite structures, where epitaxial and amorphous BSTs act as a ferroelectric and low-K dielectric component. The amorphous BST suppressed the effective permittivity of the composite capacitor, while the epitaxial BST contributed to the tunability keeping it nearly as large as that of the epitaxial BST film.

4. Conclusions

For the improved tunable performance of BST films, we have investigated new type of growth processes utilizing the amorphous BST thin layer. In the first approach, two-step growth realized an effective strain relaxation in the epitaxial films through the epitaxial crystallization of first amorphous thin layer. The relaxation of the compressive strain led to higher permittivity and higher tunability of the films. In the second approach, self-selective epitaxial growth realized the epitaxial/amorphous BST composite structure, where the first amorphous thin layer was used for blocking the crystallization of upper BST films. This growth process allowed the self build-up of the parallel composite structure by simultaneous growth of both epitaxial/amorphous phases. Keeping the deterioration of tunability to a minimum, great reduction of the effective permittivity was achieved. However, the proposed methods are not fully developed for practical application at this time. Therefore, there are still questions and issues for the use of amorphous thin layers in the property control of tunable ferroelectric films. For instance, selective epitaxial growth process should be applied to other epitaxial electrode/substrate systems compatible with microwave devices. Nevertheless, the results obtained here give us an idea about the capability of BST thin films as a tunable element without using other materials for property control.

Acknowledgments

This work was supported by the Swiss National Science Foundation and EU 6th FP projects—RETINA and NANOSTAR. The authors thank Mr. R. Gysel for AFM measurement.

References

1. Vendik, O. G., Hollman, E. K., Kozyrev, A. B. and Prudan, A. M., Ferroelectric tuning of planar and bulk microwave devices. *J. Supercond.*, 1999, **12**, 325–338.
2. Tagantsev, A. K., Sherman, V. O., Astafiev, K. F., Venkatesh, J. and Setter, N., Ferroelectric materials for microwave tunable applications. *J. Electroceram.*, 2003, **11**, 5–66.
3. Astafiev, K. F., Sherman, V. O., Tagantsev, A. K., Setter, N., Rivkin, T. and Ginley, D., Investigation of electrical degradation effects in ferroelectric thin film based tunable microwave components. *Integr. Ferroelectr.*, 2002, **49**, 103–112.
4. Pertsev, N. A., Tagantsev, A. K. and Setter, N., Phase transitions and strain-induced ferroelectricity in $SrTiO_3$ epitaxial thin films. *Phys. Rev. B*, 2000, **61**, R825–R829.
5. Haeni, J. H., Irvin, P., Chang, W., Uecker, R., Reiche, P., Li, Y. L. *et al.*, Room-temperature ferroelectricity in strained $SrTiO_3$. *Nature*, 2004, **430**, 758–761.
6. Yamada, T., Astafiev, K. F., Sherman, V. O., Tagantsev, A. K., Muralt, P. and Setter, N., Strain relaxation of epitaxial $SrTiO_3$ thin films on $LaAlO_3$ by two-step growth technique. *Appl. Phys. Lett.*, 2005, **86**, 142904-1–142904-3, and references therein for the coefficients used in the calculation.
7. Suzuki, T., Nishi, Y. and Fujimoto, M., Analysis of misfit relaxation in heteroepitaxial $BaTiO_3$ thin films. *Philos. Mag. A*, 1999, **79**, 2461–2483.
8. Yamada, T., Astafiev, K. F., Sherman, V. O., Tagantsev, A. K., Su, D., Muralt, P. *et al.*, Structural and dielectric properties of strain-controlled epitaxial

$SrTiO_3$ thin films by two-step growth technique. *J. Appl. Phys.*, 2005, **98**, 054105-1–054105-7.
9. Vendik, O. G., Zubko, S. P. and Nikolski, M. A., Modeling and calculation of the capacitance of a planar capacitor containing a ferroelectric thin film. *Tech. Phys.*, 1999, **44**, 349–355.
10. Sherman, V. O., Tagantsev, A. K. and Setter, N., Ferroelectric-dielectric tunable composites. *J. Appl. Phys.*, 2006, **99**, 074104-1–074104-10.
11. Lee, J.-S., Wang, H., Lee, S. Y., Foltyn, S. R. and Jia, Q. X., Lateral epitaxial growth of (Ba, Sr)TiO_3 thin films. *Appl. Phys. Lett.*, 2003, **83**, 5494–5496.
12. Yamada, T., Sherman, V. O., Nöth, A., Muralt, P., Tagantsev, A. K. and Setter, N., Epitaxial/amorphous $Ba_{0.3}Sr_{0.7}TiO_3$ film composite structure for tunable applications. *Appl. Phys. Lett.*, 2006, **89**, 032905-1–032905-3.